JOURNAL OF RESEARCH of the National Bureau of Standards—A. Physics and Chemistry
Vol. 79A, No. 1, January–February 1975

Polarization Effects on Fluorescence Measurements

E. D. Cehelnik, K. D. Mielenz, and R. A. Velapoldi

Institute for Materials Research, National Bureau of Standards, Washington, D.C. 20234

(October 19, 1974)

Polarization effects on fluorescence measurements are a function of four independent variables. The first is F, the polarization ratio of the exciting light which reaches the sample. The second is r, the emission anisotropy of the sample, which is the polarization "response" of the sample to plane polarized exciting light. The third is G, the polarization ratio of the emission detection system, which is the ratio of the sensitivities of the detection system to vertically and horizontally polarized light. The fourth is α, the viewing angle, which is the angle between the direction of the propagation of the exciting light and the direction from which the emission is being detected.

The intensity and the degree of polarization of the fluorescence emission that the sample exhibits are functions of F, r, and α, while the actual readings obtained with a typical spectrofluorimeter are functions of all four variables, F, r, α, and G. A theoretical analysis is made taking all these factors into account, and proper mathematical models are developed for the different modes of operation in which a fluorimeter can be used. These are verified experimentally with data obtained for a sample which has a high degree of emission anisotropy (Nile Blue A Perchlorate in glycerol). A recently designed goniospectrofluorimeter was used. Calibration procedures are developed and recommendations are made for modes of operation and fluorescence standards.

Key words: Emission anisotropy; fluorescence; fluorescence quantum yield; fluorescence standards; fluorimetry; polarization; spectrofluorimetry; viewing angle.

1. Introduction

The measurement of fluorescence polarization is an important analytical technique in identifying molecular transitions and obtaining information on the structure of macromolecules. Polarization of fluorescence also constitutes a significant source of systematic errors in fluorescence intensity measurements, such as; measurements of excitation and emission spectra, relative quantum yield determinations, and fluorescence decay measurements. All of these measurements are fraught with experimental difficulties in that the intensity readings and the apparent degree of polarization of the fluorescence emission from a polarizing sample depend, not only on the emission anisotropy of the sample itself, but also on the state of polarization of the exciting radiation and on polarization effects introduced by the sample cell and the emission detection system. These instrumental artifacts have been considered by several authors. Weber and Teale [1][1] derived an equation for obtaining fluorescence quantum yields based on a solution scatterer as the standard. This equation is valid when the excitation is unpolarized and contains a correction factor that takes into account the polarizations of the sample and the standard. Azumi and McGlynn [2] developed a technique to obtain the correction factor required to eliminate the bias of the emission detection system with respect to the state of polarization of the fluorescence emission. This factor is obtained by successive measurements with a polarizer in the emission beam alined in the vertical and horizontal positions, and a polarizer alined horizontally in the excitation beam. For the spectral calibration of the emission detection system, Melhuish [3] used a magnesium-oxide scatterer to depolarize the incident radiation, and a polarizer at the entrance slit of the emission monochromator. True spectra are obtained by recording spectra with the polarizer in the vertical and horizontal positions, applying the appropriate correction factors, and adding. Whereas these authors use right-angle viewing, Almgren [4] and Shinitzky [5] pointed out that the fluorescence emission from a polarized sample displays a typical anisotropic distribution which may make it desirable to use a different viewing angle. Assuming unpolarized exciting radiation, they showed theoretically that the fluorescence intensity is unaffected by the emission anisotropy of the sample if a viewing angle of $\cos^{-1}\sqrt{1/3}$ is chosen.

In this paper we attempt to give a unified picture of the combined effects of sample emission anisotropy and spectrofluorimeter polarization properties on fluorescence intensity and polarization measurements. A theoretical analysis is made of the general case in which a sample having nonzero emission anisotropy is excited by partially polarized radiation, and is analyzed with a biased detection system at arbitrary

[1] Figures in brackets indicate the literature references at the end of this paper.

viewing angles. This analysis is reduced to proper mathematical models for the different modes of operation in which a fluorimeter can be used, and is verified experimentally. Calibration procedures are developed and recommendations are made for various modes of operation and uses of fluorescence standards.

2. Theory

Polarization of fluorescence indicates that the emission dipoles of the excited molecules are preferentially oriented with respect to the electric vector of the exciting radiation. This usually occurs when relatively large molecules with long molecular axes have short fluorescence lifetimes relative to their rotational relaxation times, so that after excitation these molecules emit before they can rotate sufficiently to lose all 'memory' of the exciting field.

The general expressions for this anisotropic distribution of emitting molecules are obtained as follows [6]. Referring to figure 1, we assume that the exciting

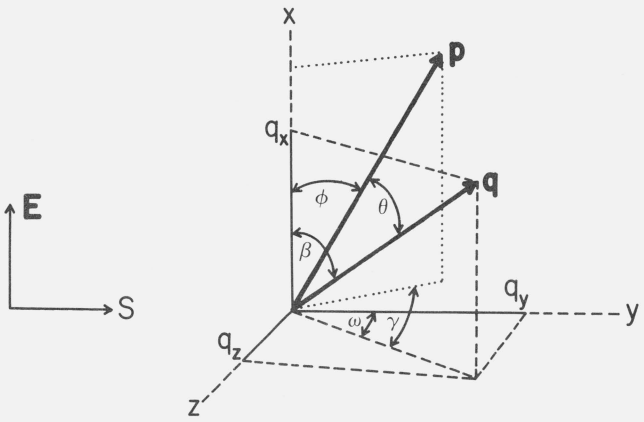

FIGURE 1. *Spatial orientation of the absorption and emission probability vectors,* **p** *and* **q,** *of a randomly oriented molecule relative to the electric vector,* **E,** *of the exciting radiation which propagates along the* y *axis with photon flux density,* S.

The emission probability vector has been resolved into the components q_x, q_y, and q_z along the x, y, and z axes. The coordinate system is the same as in ref. [5].

radiation is plane polarized with its electric vector **E** parallel to the x axis, and that it is propagating in the y direction with a photon flux density S ($h\nu$ cm^{-2} s^{-1}) [7]. This radiation field interacts with a randomly oriented collection of molecules with absorption and emission dipole oscillators that have fixed orientations relative to the molecular structure and enclose a given angle θ, as shown in figure 1. The probabilities for absorption and emission by one arbitrarily oriented molecule are given by the squared magnitudes of the probability vectors **p** and **q,** so that

$$|\mathbf{p}|^2 = S\sigma_0 \cos^2 \phi, \tag{1a}$$

$$|\mathbf{q}|^2 = Q|\mathbf{p}|^2, \tag{1b}$$

where ϕ is the angle between the absorption oscillator and the electric field, σ_0 is the absorption cross section for absorption oscillators which are parallel to the electric field of the exciting radiation, and Q is the quantum efficiency for fluorescence. The squared components of **q** in the directions of the three coordinate axes are:

$$q_x^2 = |\mathbf{q}|^2 \cos^2 \beta = S\sigma_0 Q \cos^2 \phi \cos^2 \beta, \tag{2a}$$

$$q_y^2 = |\mathbf{q}|^2 \sin^2 \beta \cos^2 \omega = S\sigma_0 Q \cos^2 \phi \sin^2 \beta \cos^2 \omega, \tag{2b}$$

$$q_z^2 = |\mathbf{q}|^2 \sin^2 \beta \sin^2 \omega = S\sigma_0 Q \cos^2 \phi \sin^2 \beta \sin^2 \omega, \tag{2c}$$

where β is given by

$$\cos \beta = \cos \theta \cos \phi + \sin \theta \sin \phi \cos \gamma, \tag{3}$$

γ being the angle between the planes **(E, p)** and **(E, q).**

The corresponding expressions for a random collection of molecules are obtained by substituting the appropriate averages of the various trigonometric functions into these equations. Since the number of absorption oscillators in a solid angle element in the direction ϕ is proportional to $d(\cos \phi)$, we have

$$\overline{\cos^{2n} \phi} = \int_0^{\pi} \cos^{2n} \phi \, d(\cos \phi) \Big/ \int_0^{\pi} d(\cos \phi)$$

$$= 1/(2n+1). \tag{4a}$$

On the other hand, the distribution of molecules is isotropic in γ and ω, so that

$$\overline{\cos \gamma} = \int_0^{2\pi} \cos \gamma d\gamma \Big/ \int_0^{2\pi} d\gamma = 0, \tag{4b}$$

$$\overline{\cos^2 \gamma} = \int_0^{2\pi} \cos^2 \gamma d\gamma \Big/ \int_0^{2\pi} d\gamma = 1/2, \tag{4c}$$

and similarly

$$\overline{\cos^2 \omega} = \overline{\sin^2 \omega} = 1/2. \tag{4d}$$

Therefore,

$$\overline{\cos^2 \phi \cos^2 \beta} = \overline{\cos^2 \theta}\ \overline{\cos^4 \phi} + \overline{\sin^2 \theta}\ \overline{\cos^2 \phi \sin^2 \phi}\ \overline{\cos^2 \gamma} + 2\ \overline{\cos \theta \sin \theta \cos^3 \phi \sin \phi}\ \overline{\cos \gamma}$$

$$= \overline{\cos^2 \theta}\ \overline{\cos^4 \phi} + (1/2)\ \overline{\sin^2 \theta}\ (\overline{\cos^2 \phi} - \overline{\cos^4 \phi})$$

$$= (1/5)\ \overline{\cos^2 \theta} + (1/15)\ \overline{\sin^2 \theta}$$

$$= (1/15)\ (2\ \overline{\cos^2 \theta} + 1), \tag{5a}$$

and

$$\overline{\cos^2 \phi \sin^2 \beta \cos^2 \omega} = \overline{\cos^2 \phi \sin^2 \beta \sin^2 \omega}$$

$$= (1/2)\,\overline{\cos^2\phi \sin^2\beta}$$

$$= (1/2)\,(\overline{\cos^2\phi}$$

$$- \overline{\cos^2\phi \cos^2\beta})$$

$$= (1/2)[(1/3)$$

$$- (1/15)(2\,\overline{\cos^2\theta} + 1)]$$

$$= (1/15)(2 - \overline{\cos^2\theta}). \quad (5b)$$

Hence, eqs (1a, b) and (2a, b, c) lead to

$$\overline{|\mathbf{p}|^2} = (1/3) S\sigma_0, \quad (6a)$$

$$\overline{|\mathbf{q}|^2} = (1/3) S\sigma_0 Q, \quad (6b)$$

$$\overline{q_x^2} = (1/15) S\sigma_0 Q (2\,\overline{\cos^2\theta} + 1), \quad (6c)$$

$$\overline{q_y^2} = \overline{q_z^2} = (1/15) S\sigma_0 Q (2 - \overline{\cos^2\theta}). \quad (6d)$$

In order to relate these results to the macroscopic properties of the sample, consider a volume element $dV = dxdydz$ containing dN molecules. The photon flux ($h\nu$ s^{-1}) into this volume element is

$$d\Phi_0 = S dx dz, \quad (7a)$$

and, according to eq (6a), the absorbed flux is

$$d\Phi_a = |p|^2 dN = (1/3) S\sigma_0 dN$$
$$= d\Phi_0 (1/3)\sigma_0 (dN/dV)\, dy. \quad (7b)$$

The analogous expression given by Beer's law is

$$d\Phi_a = d\Phi_0 (\ln 10)\, \epsilon c dy, \quad (7c)$$

where ϵ is the molar absorptivity (l mol^{-1} cm^{-1}) and c is the concentration (mol l^{-1}). If dV is measured in cm^3, we have $dN/dV = c\mathfrak{N}/1000$ (where $\mathfrak{N}$ is Avogadro's number) and therefore

$$\sigma = (1/3)\sigma_0 = \left[\frac{1000 (\ln 10)}{\mathfrak{N}}\right] \epsilon. \quad (8a)$$

Here, σ represents the average absorption cross section (in cm^2) per molecule [8]. Similarly

$$\tau = \sigma Q = \left[\frac{1000 (\ln 10)}{\mathfrak{N}}\right] \epsilon Q, \quad (8b)$$

is the corresponding cross section for fluorescence. Equations (6a, b) may then be expressed in the forms

$$\overline{|\mathbf{p}|^2} = S\sigma, \; \overline{|\mathbf{q}|^2} = S\tau, \quad (9a)$$

and by analogy eqs (6c, d) become

$$\overline{q_x^2} = S\tau_{||}, \; \overline{q_y^2} = \overline{q_z^2} = S\tau_\perp, \quad (9b)$$

where

$$\tau_{||} = (1/5)\tau(\overline{2\cos^2\theta} + 1), \quad (10a)$$

and

$$\tau_\perp = (1/5)\tau(2 - \overline{\cos^2\theta}), \quad (10b)$$

are identified as the component cross sections for molecules with absorption dipole oscillators that are parallel and perpendicular, respectively, to the electric field vector of the exciting radiation. Alternative forms of eqs (10a, b) which are useful for mathematical convenience, are

$$\tau_{||} = (1/3)\tau(1 + 2r), \quad (11a)$$

$$\tau_\perp = (1/3)\tau(1 - r), \quad (11b)$$

where

$$r = \frac{\tau_{||} - \tau_\perp}{\tau} = (1/5)\,(\overline{3\cos^2\theta} - 1), \quad (12)$$

is the 'emission anisotropy' of the sample, as defined by Jablonski [9].

For a collection of randomly oriented molecules that do not rotate during the time interval between absorption and emission (a 'random but frozen' distribution), θ is constant and equal to the intramolecular angle of energy transfer between the absorption and emission dipoles, θ_0. In this case, eq (12) defines the intrinsic emission anisotropy of the molecule,

$$r_0 = (1/5)\;(3\cos^2\theta_0 - 1). \quad (13a)$$

The range of possible values for r_0 is

$$-0.2 \leq r_0 \leq 0.4, \quad (13b)$$

where the two limiting cases are those in which the absorption and emission dipoles are either parallel ($r_0 = 0.4$) or perpendicular ($r_0 = -0.2$) to each other. In a random aggregate of mobile emission oscillators, each molecule rotates over a certain angle θ' between absorption and emission. In this case the angle θ appearing in eq (12) is given by an expression similar to eq (3); that is,

$$\cos\theta = \cos\theta_0 \cos\theta' + \sin\theta_0 \sin\theta' \cos\gamma', \quad (14a)$$

where γ' is the angle between the two planes defined by the absorption and emission oscillators at the times of absorption and emission. As in the case of eqs (4b, c), we have

$$\overline{\cos\gamma'} = 0, \; \overline{\cos^2\gamma'} = 1/2,$$

and therefore

$$\overline{\cos^2\theta} = \cos^2\theta_0\,\overline{\cos^2\theta'} + (1/2)\,\sin^2\theta_0\,\overline{\sin^2\theta'}. \quad (14b)$$

This can be rearranged to give

$$(3\,\overline{\cos^2\theta} - 1) = (1/2)\,(3\cos^2\theta_0 - 1)\,(3\,\overline{\cos^2\theta'} - 1), \quad (14c)$$

so that

$$r = (1/2)\,r_0\,(3\,\overline{\cos^2\theta'} - 1). \quad (14d)$$

Thus, $r = 0$ for a completely relaxed system for which the fluorescence lifetime is significantly longer than the rotational relaxation time of the molecules, so that the distribution in θ' becomes random (i.e., $\overline{\cos^2\theta'} = 1/3$). The intermediate cases in which the randomization due to Brownian motion or intermolecular energy transfer is only partially effective ($\overline{\cos^2\theta'} > 1/3$) lead to values of $r \neq 0$ within a narrower range than that specified in (13b).

The fluorescence emission detected when a sample with given emission anisotropy r is analyzed with a typical spectrofluorimeter can now be calculated in the following manner, which is a generalization of the treatments given by Kalantar [10], Almgren [4], and Shinitzky [5]. As depicted in figure 2, the exciting radiation is assumed to be partially polarized and is regarded as the incoherent superposition of two plane-polarized components with photon flux densities, S^V and S^H, which are propagated in the y direction, and with electric vectors, $\mathbf{E}^V$ and $\mathbf{E}^H$, which are parallel to the x and z directions, respectively. The anisotropic distribution of emission dipoles is again described in terms of a probability vector $\mathbf{q}$, which is similarly regarded as the incoherent superposition of two vectors, $\mathbf{q}^V$ and $\mathbf{q}^H$. The components of the latter with respect to the three coordinate axes are obtained from eq (9b), once directly and once with interchanged x and z coordinates. Thus, the rms components of $\mathbf{q}$ are given by

$$\overline{q_x^2} = S^V\tau_{\parallel} + S^H\tau_{\perp}, \quad (15a)$$

$$\overline{q_y^2} = S^V\tau_{\perp} + S^H\tau_{\perp}, \quad (15b)$$

$$\overline{q_z^2} = S^V\tau_{\perp} + S^H\tau_{\parallel}. \quad (15c)$$

The fluorescence intensity $I(\alpha)$ ($h\nu\,s^{-1}\,sr^{-1}$) emitted into a given viewing direction α in the yz plane is proportional to the squared rms components of $\mathbf{q}$ in the plane perpendicular to this viewing direction and is polarized in the directions of these components. Thus it is seen that $I(\alpha)$ consists of vertically and horizontally polarized components which are proportional to q_x^2 and ($q_y^2\,\sin^2\alpha + q_z^2\,\cos^2\alpha$), respectively. When eqs (15a, b, c) and (11a, b) are used to evaluate these expressions, it is seen that $I(\alpha)$ is the sum of the four components

$$I_V^V(\alpha) = kS^V\tau_{\parallel} = (1/3)kS^V\tau(1+2r), \quad (16a)$$

$$I_V^H(\alpha) = kS^H\tau_{\perp} = (1/3)kS^H\tau(1-r), \quad (16b)$$

$$I_H^V(\alpha) = kS^V\tau_{\perp} = (1/3)kS^V\tau(1-r), \quad (16c)$$

$$\begin{aligned} I_H^H(\alpha) &= kS^H(\tau_{\perp}\sin^2\alpha + \tau_{\parallel}\cos^2\alpha) \\ &= (1/3)kS^H\tau[(1-r) + 3r(\cos^2\alpha)]. \end{aligned} \quad (16d)$$

where k is an appropriate constant of proportionality. (Here, as in similar equations to be developed later on, superscripts refer to the state of polarization of the exciting radiation, and subscripts refer to the state of polarization of the emitted flux. The letters V and H denote vertically and horizontally polarized light, and similarly the letter U will be used to denote unpolarized light. No sub- or superscripts refer to the general case of partial polarization.)

The fluorescence intensities emitted along the three coordinate axes in figure 2 are

$$I_x = k\,(\overline{q_y^2} + \overline{q_z^2}),\ I_y = k\,(\overline{q_z^2} + \overline{q_x^2}),\ I_z = k\,(\overline{q_x^2} + \overline{q_y^2}). \quad (17a)$$

Therefore,

$$\begin{aligned} I_0 &\equiv (1/3)(I_x + I_y + I_z) = (2/3)\,k\,(\overline{q_x^2} + \overline{q_y^2} + \overline{q_z^2}) \\ &= (2/3)k(S^V + S^H)\ (\tau_{\parallel} + 2\tau_{\perp}) \\ &= (2/3)k(S^V + S^H)\tau, \end{aligned} \quad (17b)$$

represents the spatial average of the intensity emitted by the sample. This average intensity I_0 (which is equal to the intensity that would be emitted into any

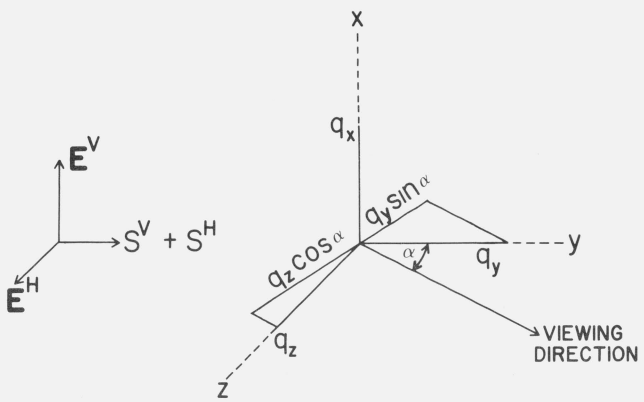

FIGURE 2. *Resolution of the emission probability vector,* $\mathbf{q}$, *into components:*

(a) q_x, q_y, q_z—*Components parallel and perpendicular to the electric field vectors,* $\mathbf{E}^V$ *and* $\mathbf{E}^H$ *of partially polarized exciting radiation with a photon flux density of* $S^V + S^H$, *and*

(b) (q_z *cos* α) *and* (q_y *sin* α)—*components perpendicular to the viewing angle,* α.

viewing direction if the sample had zero emission anisotropy) is proportional to the fluorescence quantum yield of the sample, and therefore constitutes a physically meaningful basis for fluorescence measurements. Thus, the bias introduced into fluorescence intensity measurements by the emission anisotropy r of a sample is revealed by combining eqs (16a–16d) and (17b) to give.

$$I(\alpha) = I_V^V(\alpha) + I_H^V(\alpha) + I_V^H(\alpha) + I_H^H(\alpha)$$

$$= I_0 \left\{ 1 + r \left[\frac{3\cos^2\alpha + (F-2)}{2(1+F)} \right] \right\}, \quad (18)$$

where

$$F \equiv S^V/S^H, \quad (19)$$

is the polarization ratio of the exciting radiation. In addition, eqs (16a–16d) show that the degree of polarization of the fluorescence emission,

$$P(\alpha) \equiv \frac{[I_V^V(\alpha) + I_V^H(\alpha)] - [I_H^V(\alpha) + I_H^H(\alpha)]}{[I_V^V(\alpha) + I_V^H(\alpha)] + [I_H^V(\alpha) + I_H^H(\alpha)]}$$

$$= \frac{3r(F - \cos^2\alpha)}{2(1+F) + r[3\cos^2\alpha + (F-2)]}, \quad (20)$$

is also a rather complicated function of emission anisotropy, polarization of the exciting radiation, and viewing geometry.

These results lead to several important conclusions for the particular cases in which the exciting radiation is either plane polarized or completely depolarized. These limiting cases will be discussed now.

(a) Vertically polarized excitation ($F = \infty$). In this case,

$$I^V = I_0^V(2+r)/2, \quad (21a)$$

$$P^V = 3r/(2+r), \quad (21b)$$

where the argument α is omitted since these expressions are independent of viewing angle. These two equations can be combined into

$$I^V = 3I_0^V/(3 - P^V), \quad (21c)$$

which is valid for arbitrary viewing angles α. Similarly eqs (21b) and (10a, b) show that the well-known relation

$$P^V = \frac{\tau_{\parallel} - \tau_{\perp}}{\tau_{\parallel} + \tau_{\perp}} = \frac{3\overline{\cos^2\theta} - 1}{3 + \overline{\cos^2\theta}}, \quad (21d)$$

is also valid for all values of α ($P_0^V = 1/2$ or $-1/3$ for $\theta_0 = 0$ and 90°, respectively). This independence of viewing angle and, thus, insensitivity to misalinement, as well as the simplicity of eqs (21c, d) make vertically polarized excitation a particularly desirable mode of operation of a fluorimeter.

(b) Horizontally polarized excitation ($F = 0$). Here, eqs (18) and (20) are reduced to

$$I^H(\alpha) = I_0^H[1 + (1/2)r(3\cos^2\alpha - 2)], \quad (22a)$$

$$P^H(\alpha) = \frac{-3r(\cos^2\alpha)}{2 + r(3\cos^2\alpha - 2)}, \quad (22b)$$

which shows that both quantities vary with viewing angle. A useful fact is that at the usual right angle viewing geometry of common fluorimeters $P^V(90°) = 0$, and thus the fluorescence emission is unpolarized. As pointed out by Azumi and McGlynn [2], this property of the horizontally polarized mode of excitation can be employed for the polarization calibration of emission monochromators.

(c) Unpolarized excitation ($F = 1$). In this case, one obtains

$$I^U(\alpha) = I_0^U[1 + (1/4)r(3\cos^2\alpha - 1)], \quad (23a)$$

$$P^U(\alpha) = \frac{3r(\sin^2\alpha)}{4 + r(3\cos^2\alpha - 1)}. \quad (23b)$$

Equation (23a) constitutes the basis for the previously mentioned proposal to use $\alpha_d = \cos^{-1}\sqrt{1/3}$ as the preferred viewing angle for which the fluorescence intensity, $I^U(\alpha_d) = I_0$, is unaffected by the emission anisotropy of the sample. Equation (23b) shows that $P^U(\alpha_d) = 1/2\ r$, which constitutes another interesting and not previously noted property of this particular viewing geometry. It should be noted, however, that

$$I^U(\alpha_d + \Delta\alpha) = I_0^U(1 - r\Delta\alpha/\sqrt{2} + \ldots), \quad (23c)$$

and

$$P^U(\alpha_d + \Delta\alpha) = (1/2)\ r\ [1 + (1+r)\ \Delta\alpha/\sqrt{2} + \ldots], \quad (23d)$$

which indicate that both conditions are sensitive to angular misalinements. For example, a 1° departure from α_d will produce a 0.5 percent error in $I^U(\alpha)$ and a 1.8 percent error in $P^U(\alpha)$ if $r = 0.4$. The common 90° geometry of ordinary fluorimeters is less sensitive to errors in angular alinement, since eqs (18) and (20) both have zero derivatives for $\alpha = 90°$.

For right-angle viewing, eqs (23a, b) are reduced to

$$I^U(90°) = I_0^U(4-r)/4, \quad (24a)$$

$$P^U(90°) = 3r/(4-r), \quad (24b)$$

which can be combined into the familiar form used in the Weber-Teale correction formula [1],

$$I^U(90°) = 3\,I_0^U/[3 + P^U(90°)]. \quad (24c)$$

Equations (24b) and (10a, b) also show that

$$P^U(90°) = \frac{\tau_{||} - \tau_\perp}{\tau_{||} + 3\tau_\perp} = \frac{3\,\overline{\cos^2\theta} - 1}{7 - \overline{\cos^2\theta}}, \qquad (24d)$$

which is another well-known expression ($P_0^U(90°) = 1/3$ and $-1/7$ for $\theta_0 = 0°$ and 90°, respectively). These equations are valid for right-angle viewing, only.

The preceding discussion is summarized in figures 3 and 4, which show plots of florescence intensity and degree of polarization versus viewing angle for the three modes of excitation assumed and for $r = 0.383$. In the Discussion Section, these graphs will be compared with experimental data.

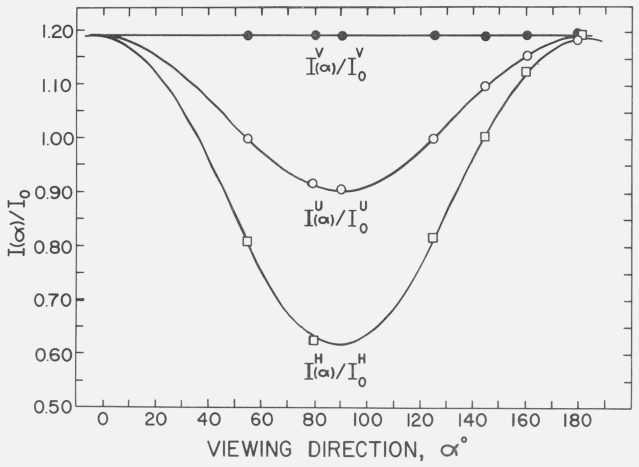

FIGURE 3. *Ratio of the fluorescence intensities for vertically* $\left(\frac{I^V(\alpha)}{I_0^V}\right)$, *horizontally* $\left(\frac{I^H(\alpha)}{I_0^H}\right)$, *and depolarized* $\left(\frac{I^U(\alpha)}{I_0^U}\right)$ *exciting radiation.*

The numerators are the intensities emitted by an anisotropic sample into the viewing angle, α and the denominators are the corresponding intensities of a sample having zero emission anisotropy. The solid lines represent theoretical curves and the symbols represent values obtained from experimental data.

In addition to providing partially polarized exciting radiation, most fluorimeters also have a detection system which is biased to the polarization of the fluorescence emission. Thus, the recorded signals corresponding to the four components of the fluorescence intensity given by eqs (16a–16d) are

$$R_V^V(\alpha) = T_V I_V^V(\alpha) = kS^V\tau_{||}T_V$$
$$= (1/3)kS^V\tau(1+2r)T_V, \qquad (25a)$$

$$R_V^H(\alpha) = T_V I_V^H(\alpha) = kS^H\tau_\perp T_V$$
$$= (1/3)kS^H\tau\,(1-r)\,T_V, \qquad (25b)$$

$$R_H^V(\alpha) = T_H I_H^V(\alpha) = kS^V\tau_\perp T_H$$
$$= (1/3)kS^V\tau\,(1-r)T_H, \qquad (25c)$$

$$R_H^H(\alpha) = T_H I_H^H(\alpha) = kS^H\,(\tau_\perp \sin^2\alpha + \tau_{||}\cos^2\alpha)\,T_H$$
$$= (1/3)\,kS^H\tau\,[(1-r) + 3r\,(\cos^2\alpha)]\,T_H, \qquad (25d)$$

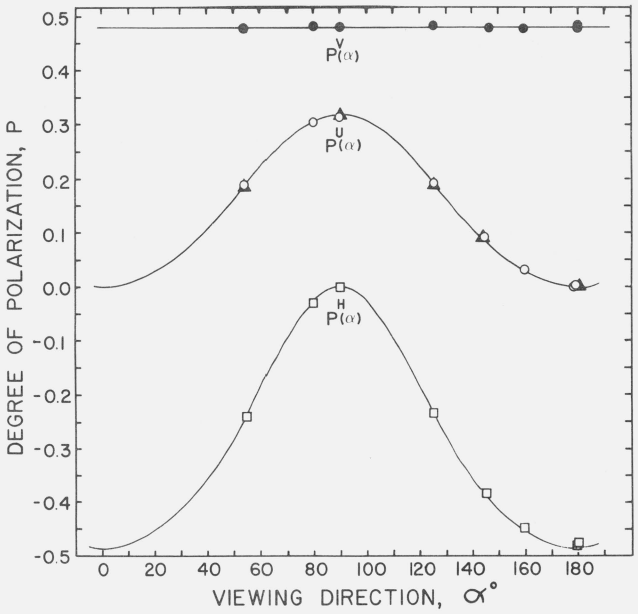

FIGURE 4. *The degree of polarization,* P, *for vertically* $[P^V(\alpha)]$, *horizontally* $[P^H(\alpha)]$, *and depolarized* $[P^U(\alpha)]$ *exciting radiation as a function of viewing angle.*

The solid lines represent theoretical curves and the symbols represent values obtained from experimental data.

where T_V and T_H are the sensitivities of the detection system for vertically and horizontally polarized radiation, respectively. Similarly, the signal corresponding to the (unpolarized) spatial average I_0 of the fluorescence intensity is

$$R_0 = (1/2)\,(T_V + T_H)I_0 = (1/3)k(S^V + S^H)\tau(T_V + T_H). \qquad (26)$$

Combining these equations gives

$$R(\alpha) = R_V^V(\alpha) + R_V^H(\alpha) + R_H^V(\alpha) + R_H^H(\alpha)$$
$$= R_0\left\{1 + r\left[\frac{3\cos^2\alpha - (1+F+G-2FG)}{(1+F)(1+G)}\right]\right\}, \qquad (27)$$

where $R(\alpha)$ is the total signal recorded, and where

$$G \equiv T_V/T_H, \qquad (28)$$

is the polarization ratio of the detection system.

Equation (27) is analogous to eq (18), and describes the combined polarization effects of sample, exciting radiation, viewing angle, and detection system. It reduces to eq. (23a) if $F = G = 1$, and shows that the general condition for which $R(\alpha) = R_0$ is given by

$$\cos^2\alpha = (1/3)\,(1+F+G-2FG). \qquad (29)$$

However, the angle so defined depends on the polarization ratios of the exciting radiation and the detection

system, and therefore is different for different fluorimeters, and for the same fluorimeter the angle varies with excitation and emission wavelengths. Furthermore, no real solution at all is obtained for α unless $0 \leq 1+F+G-2FG \leq 3$. Hence it is seen that, under typical laboratory conditions, there is no practicable viewing geometry for which the recorded signal is an unbiased measure of the quantum efficiency of a sample having a nonzero emission anisotropy r. In order to utilize the effect predicted by Almgren [4] and Shinitzky [5], it is necessary to depolarize the excitation and detection systems by using scrambler plates in both beams. However, most spectrofluorimeters cannot easily be adapted to provide the 54.75° or 125.25° viewing geometry required in this case. Furthermore, no information can be obtained about the emission anisotropy of the sample unless readings are also taken at other viewing angles, as will be shown.

A preferable approach is to use a fixed viewing geometry with polarizers in the excitation and emission beams. Taking the four readings defined by eqs (25a–25d) and forming the following ratios, one obtains

$$\frac{R_V^V(\alpha)}{R_H^V(\alpha)} = DG, \tag{30a}$$

$$\frac{R_H^V(\alpha)}{R_V^H(\alpha)} = F/G, \tag{30b}$$

$$\frac{R_H^H(\alpha)}{R_V^V(\alpha)} = [\cos^2\alpha + (1/D)\sin^2\alpha]/FG, \tag{30c}$$

where

$$D \equiv \tau_{\|}/\tau_{\perp}, \tag{31a}$$

is the 'dichroic ratio of emission' of the excited molecules. This quantity D is more convenient to work with than the emission anisotropy r, and is related to r by

$$D = \frac{1+2r}{1-r}, \qquad r = \frac{D-1}{D+2}. \tag{31b}$$

The possible range of values for D, as defined by eqs (13b) and (31b) is

$$1/2 \leq D \leq 3, \tag{31c}$$

with $D=1$ for an unpolarized sample. For arbitrary viewing angles α, G can be obtained by combining eqs (30a, 30b, 30c) to give

$$G^2\left[\frac{R_H^V(\alpha)}{R_V^H(\alpha)}\right]\left[\frac{R_H^H(\alpha)}{R_V^V(\alpha)}\right] - G\left[\frac{R_H^V(a)}{R_V^V(\alpha)}\right](\sin^2\alpha) - \cos^2\alpha = 0. \tag{32a}$$

Solving this quadratic gives

$$G = \left[\frac{R_V^H(\alpha)}{R_H^H(\alpha)}(\sin^2\alpha)/2\right] + \sqrt{\left[\frac{R_V^H(\alpha)}{R_H^H(\alpha)}(\sin^2\alpha)/2\right]^2 + \left[\frac{R_V^H(\alpha)}{R_H^H(\alpha)}\right]\left[\frac{R_V^V(\alpha)}{R_H^V(\alpha)}\right](\cos^2\alpha)}, \tag{32b}$$

where only the positive root has physical significance. With G determined, F and D are obtained from eqs (30a, 30b), so that the desired unbiased reading R_0 can now be found from the four individual readings in several different ways. A useful expression for R_0, which is independent of viewing angle, is obtained by combining eqs (25a, 25b, 25c) into

$$\frac{R_V^V(\alpha)}{S^V T_V} + \frac{R_V^H(\alpha)}{S^H T_V} + \frac{R_H^V(\alpha)}{S^V T_H} = k\tau. \tag{33a}$$

Upon substitution into eq (26), this leads to

$$R_0 = \frac{(1+F)(1+G)}{3FG}[R_V^V(\alpha) + FR_V^H(\alpha) + GR_H^V(\alpha)]. \tag{33b}$$

From this discussion, it is evident that the use of polarizers in the excitation and emission beams permits the complete characterization of sample and spectrofluorimeter, and yields more information than a system not using polarizers. Equations (30a) through (33b) are applicable for arbitrary viewing angles α but give the most accurate results for $\alpha = 90°$, where the angular variation of $R_H^H(\alpha)$ is smallest. For this preferred and most commonly used viewing geometry, eq (32b) is reduced to the correction formula used by Azumi and McGlynn [2] and one obtains

$$F = \frac{R_H^V(90°)}{R_H^H(90°)}, \tag{34a}$$

$$G = \frac{R_V^H(90°)}{R_H^H(90°)}, \tag{34b}$$

$$D = \frac{R_V^V(90°)R_H^H(90°)}{R_H^V(90°)R_V^H(90°)}, \tag{34c}$$

R_0 being the same as given by eq (33b).

3. Experimental Procedures [11]

Inherent in the derivation above are the assumptions that the sample is irradiated by a parallel beam of light and that the luminescence occurs from essentially a point source. The first condition is achieved experimentally by proper alinement of the optics and the second by working with small and dilute samples

so that the low light absorption approximation of Beer's law,

$$\Phi_a = \Phi_0(1 - e^{-2.303\epsilon bc}) \simeq \Phi_0 2.303\epsilon bc,$$

is valid. The system used to investigate the polarization effects consists of a fluorescent dye dissolved in the highly viscous solvent glycerol. Exciting light at 632.8 nm is absorbed by the dye and its fluorescence at 685.0 nm was measured as a function of angle relative to the direction of propagation of the exciting light. The measurements were made using a new goniospectroradiometer recently designed and built at NBS [12]. This versatile instrument can be operated in different modes, one of which is as a spectrofluorimeter. Basically, it consists of a xenon arc source, excitation monochromator, reference detector, sample compartment, emission monochromator, signal detector, and computer-interfaced electronics. The whole emission detection system is mounted on a rotary carriage which pivots about the center line of the sample, thus allowing for viewing the sample from arbitrary angles relative to the direction of the exciting radiation between 180° (straight through) and approximately 20°.

A scale diagram of the apparatus, as adapted for this experiment, is shown in figure 5. The xenon arc source, excitation monochromator, and reference detector were removed and replaced with a 15 milliwatt He-Ne laser (HNL), a light source of high intensity and monochromaticity. The 632.8 nm laser light is reflected from a flat mirror (FM) and impinges on a barium sulfate scatterer (B) at an angle 45° from normal. A certain solid angle of the diffusely reflected light is collected and focused by the biconvex lens (L) (45 mm diam., 148 mm f.l.) through a Glan-Taylor polarizing prism (P) to the sample cell (S). The position of the lens relative to the barium sulfate and sample cell was adjusted such that the beam cross section remained nearly constant in the neighborhood of the image, thus approximating a collimated beam through the sample. The laser|barium-sulfate|lens system approximates light as it would emerge from an excitation monochromator and is used to destroy the spatial coherence of the laser light while keeping the high intensity, monochromaticity and low scattered exciting light levels (of all other wavelengths) which a xenon lamp-monochromator system cannot supply. A cylindrical NMR tube with an internal diameter of 1.35 mm and an outside diameter of 5 mm was used as the sample cell. The tube was mounted in an air driven NMR sample spinner and was spun at 2,500 rpm to average out any irregularities in the glass. The beam diameter of the exciting light at the sample was 5 mm, thus giving a "glowing rod" of fluorescence 1.35 mm in diameter and 5 mm high. The absorbance of the dye was kept low ($A = 0.019$) to have a uniform emission intensity throughout the cell as the light propagated through it. A 14° cone of the fluorescence emission was focused at the monochromator entrance slit by the ellipsoidal mirror (EL). A second Glan-Taylor polarizer (P) was placed directly behind the sample (not behind the mirror, as shown inadvertently in figure 5), and a Schott RG 645 filter (F) was placed in front of the slit. The filter cut out most of the 632.8 nm exciting light but passed most of the fluo-

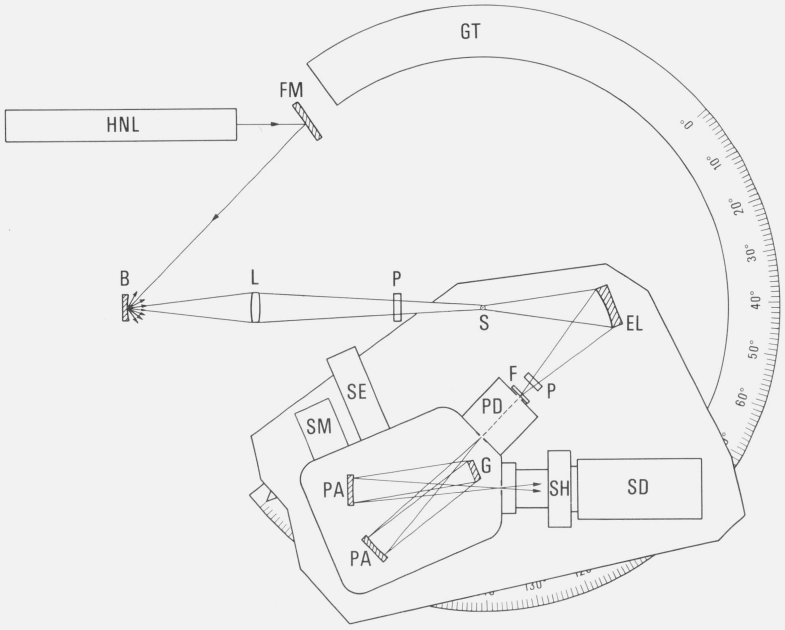

FIGURE 5. *The spectroradiometer as adapted for this experiment.*

HNL–helium neon laser; FM–flat mirror; B–barium sulfate scatterer; L–biconvex collecting lens; P–polarizer; S–spinning sample tube; EL–ellipsoidal mirror; F–Schott RG 645 filter; PD–prism predisperser; PA–G–PA–emission monochromator; SE–wavelength shaft encoder; SM–stepping motor; SH–shutter and SD–S20 photomultiplier tube. The emission detection system pivots around the sample tube on the track GT.

rescence at longer wavelengths. This made viewing at 180° (straight through) possible even though the solution absorbs only a very small percentage of the exciting light. The emission monochromator consists of a prism predisperser (PD) and a grating monochromator (PA, G, PA). The bandpass of the monochromator was 4.8 nm for the 2 mm slits which were used. The rotary table carrying the emission detection system is attached to the sample-holder support (S) by a large ball bearing, and is supported near its periphery by two rollers which move along a large circular track (GT). After the fluorescence passes through the monochromator, it was detected by an extended S–20 photomultiplier tube (SD). The signal from the PM tube was amplified and fed into a time shared computer which took a certain number of readings in a given time interval (usually 100 in 10 s). The average and the standard error were calculated and printed out on a teletype-writer. The readings were obtained in volts and the overall sensitivity of the system was adjusted by changing the dynode voltage applied to the PM tube.

Nile Blue A Perchlorate (Eastman Kodak, laser grade Lot #A3–X) was used without further purification. It was chosen because its maximum absorption band is near 632.8 nm, allowing extremely low concentrations to be used to minimize intermolecular energy transfer and self-absorption of the fluorescence which tend to depolarize the emission before it gets out of the cell. Glycerol (Fisher Certified ACS) was used as the solvent. The actual concentration of the dye used was 9.4×10^{-4} g/l (2.25×10^{-6} mol/l). No attempt was made to purge the solutions of dissolved oxygen. Blanks were run using a similar NMR tube filled with solvent only. The barium sulfate (Eastman White Reflectance Standard) was pressed into pellet form in a special holder. All measurements were carried out at room temperature, 22 °C.

4. Results

Data were taken with and without polarizers in the excitation and emission beams and at different viewing angles. With both polarizers in place, four readings were taken at each viewing angle, α, corresponding to the four different orthogonal positions the polarizers can have, $R_V^V(\alpha)$, $R_H^V(\alpha)$, $R_V^H(\alpha)$, and $R_H^H(\alpha)$ (see table 1). The superscript again refers to the mode of excitation and the subscript to the mode of the emission polarizer. The $R_H^H(\alpha)$ readings alone as a function of viewing angle α are listed in table 2. Typical standard errors of the readings of the sample and the blanks are given for the $R_H^H(\alpha)$ readings to show their magnitude and consistency as a function of the magnitude of the signal. The data are shown in the order in which they were taken and it was found that the system was stable over the time period it took to obtain a set of readings. Only a 2 or 3 percent drop in overall signal due to PM tube drift was apparent over the course of 2 hours. When the emission polarizer is removed it is only possible to take two readings at each α, $R^V(\alpha)$ and $R^H(\alpha)$. These data are shown in table 3. When the excitation polarizer is removed and the emission polarizer is left in place, again two readings are taken, $R_V(\alpha)$

TABLE 1. *Experimental readings obtained for the four orthogonal positions of the excitation and emission polarizers*

α	$R_V^V(\alpha)$	$R_H^V(\alpha)$	$R_V^H(\alpha)$	$R_H^H(\alpha)$
Degrees	*Volts*	*Volts*	*Volts*	*Volts*
180	[a] 0.2802	0.2786	0.09627	[a] 0.7795
144.75	.2814	.2798	.09772	.6092
125.25	.2817	.2781	.09739	.4436
90	.2797	.2766	.09698	.2761
54.75	.2782	.2754	.09607	.4440
180	[a] .2801	.2777	.09661	[a] .7797
160	.2821	.2796	.09688	.7163
80	.2803	.2773	.09708	.2931
Average	0.2805	0.2779	0.09688	
Std. error	0.0005	0.0005	0.0002	
% std. error	0.2	0.2	0.2	

[a] Nonzero blank subtracted from these readings.

TABLE 2. *Experimental readings for the excitation and emission polarizers in the horizontal mode as a function of viewing angle*

α	$R_H^H(\alpha)$	Std. error	Blank	Std. error blank
Degrees	*Volts*	*Volts*	*Volts*	*Volts*
180.5	0.7987	0.0038	0.0319	0.0007
175.5	.7959	.0040	.0327	.0006
170.5	.7734	.0044	.0217	.0006
165.5	.7478	.0042	.0116	.0003
160.5	.7186	.0039	.0035	.0002
155.5	.6862	.0031	.0007	.0000
150.5	.6526	.0036	.0000	.0000
145.5	.6137	.0031	.0000	.0000
140.5	.5734	.0025	.0000	.0000
135.5	.5316	.0026	.0000	.0000
130.5	.4892	.0033	.0000	.0000
125.5	.4469	.0023	.0000	.0000
120.5	.4075	.0024	.0000	.0000
115.5	.3711	.0022	.0000	.0000
110.5	.3401	.0022	.0000	.0000
105.5	.3147	.0017	.0000	.0000
100.5	.2953	.0028	.0000	.0000
95.5	.2821	.0024	.0000	.0000
90.5	.2774	.0017	.0000	.0000
85.5	.2811	.0023	.0000	.0000
80.5	.2906	.0021	.0000	.0000
75.5	.3077	.0021	.0000	.0000
70.5	.3308	.0020	.0000	.0000
65.5	.3612	.0020	.0000	.0000
60.5	.3986	.0027	.0000	.0000
55.5	.4363	.0024	.0000	.0000
50.5	.4799	.0026	.0000	.0000
45.5	.5229	.0028	.0000	.0000
180.5	.7932	.0048	.0319	.0007
125.75	.4485	.0024	.0000	.0000
55.25	.4420	.0026	.0000	.0000
54.75	.4449	.0023	.0000	.0000
125.25	.4441	.0028	.0000	.0000

TABLE 3. *Experimental readings for four different modes of spectrofluorimeter operation*

α	$R^V(\alpha)$	$R^H(\alpha)$[a]	$R_V(\alpha)$	$R_H(\alpha)$[b]	$R(\alpha)$[c]	$R_U^U(\alpha)$[d]
Degrees	*Volts*	*Volts*	*Volts*	*Volts*	*Volts*	*Volts*
180	[e]0.4955	[e]0.7977	[e]0.2829	[e]0.7981	[e]1.045	[e]0.8696
144.75	.5105	.6804	.2847	.6741	0.9043	.7826
125.25	.5207	.5295	.2855	.5495	.8029	.7096
90	.5345	.3622	.2877	.4254	.6863	.6407
54.75	.5513	.5452	.2868	.5554	.8495	.7107

[a]Polarizer in excitation beam.
[b]Polarizer in emission beam.
[c]No polarizers in excitation or emission beams.
[d]Both beams depolarized.
[e]Nonzero blanks subtracted.

and $R_H(\alpha)$ (see table 3). Also, both polarizers can be removed, as is common for most fluorimeters, and only one reading, $R(\alpha)$, can be taken at each α (see table 3). Finally, instead of placing polarizers in the excitation and emission beams, scrambler plates can be placed so as to depolarize both beams. In addition to giving unpolarized exciting light, this caused the emission detection system to see depolarized light and thus removed its bias. The scrambler plates are quartz wedges placed such that the polarized light beam is rotated different amounts depending on which part of the wedge the light is traversing. The plates therefore do not actually depolarize in the strict sense of the term, but supply to the grating strips of radiation polarized alternately parallel and perpendicular to the grating grooves [13]. Scrambler plates were placed only in the emission beam since it was found (as will be shown) that the laser|barium-sulfate|lens system supplied essentially depolarized exciting radiation. The readings taken with the scrambler plates in place, $R_U^U(\alpha)$ are also shown in table 3. It should be noted that when an optical component was removed or added, the overall sensitivity of the instrument was changed. The voltage on the PM tube was always adjusted to keep the maximum reading in a given set of readings at or below 1 volt. Therefore, only data with constant optics should be compared to each other.

5. Discussion

5.1. Excitation Polarizer In, Emission Polarizer In

The four readings $R_V^V(\alpha)$, $R_H^V(\alpha)$, $R_V^H(\alpha)$, and $R_H^H(\alpha)$ for each angle α (see table 1) are related to the intensity emitted by the sample by eqs (25a–25d). Equations (25a, 25b, 25c) predict that the $R_V^V(\alpha)$, $R_H^V(\alpha)$, and $R_V^H(\alpha)$ readings should be independent of viewing angle α. The data in table 1 show this to be true, and the average values of these readings and their standard errors are given. This shows that (a) the emission detection system collects the same solid angle at each α, (b) the rotating sample cell is uniform with respect to α, and (c) the sample is essentially a point source. The $R_H^H(\alpha)$ reading is the only one which has a dependence on α as predicted by eq (25d). Table 4 shows the values of G, F, and D calculated using eqs (32b), (30a), and (30b) and the data reported in table 1. As can be seen the values of G all agree and have an average value of 0.353. This value is what one might expect with a grating monochromator detection system viewing at 685.0 nm. The values of F agree and have an average value of 1.3 percent above unity which means that the barium sulfate scatterer is efficient in depolarizing the highly polarized He-Ne laser light, and that the sample cell transmits polarized light uniformly. The values of D are also nearly constant giving an average value of 2.86 ± 0.02. This value is close to the theoretical maximum of 3.0 (corresponding to $r_0 = 0.4$ or $P_0^V = 0.5$) for the case where the absorption and emission dipole oscillators are parallel to each other. The theoretical maximum of 3.0 is what one would expect in this case since the excitation occurs in the longest wavelength absorption band of the dye, the same state from which emission theoretically occurs. The small deviation from 3.0 is probably due to the fact that the solvent is not quite viscous enough at room temperature to completely prevent Brownian motion of the molecules during their excited state lifetime.

A value for D can also be obtained from the $R_H^H(\alpha)$ readings alone. Equation (25d) can be rearranged to give

$$R_H^H(\alpha) = k(\tau_{\parallel} - \tau_{\perp}) S^H T_H \cos^2\alpha + k\tau_{\perp} S^H T_H \,. \tag{35}$$

A plot of $R_H^H(\alpha)$ values (from table 2) versus $\cos^2\alpha$ is shown in figure 6. The slope to intercept ratio gives $D = 2.85 \pm 0.07$, which agrees well with the average value of 2.86 recorded in table 4. This shows that not only do eqs (25a–25*d*) accurately represent the data but also that the intensity effect predicted by Almgren [4], Shinitzky [5], and Kalantar [10] will be apparent once the correction factors F and G are applied. Equation (23a) can be written in terms of the experimentally obtainable readings as

$$\frac{I^U(\alpha)}{I_0^U} = (3/4)\left[1 + \frac{R_H^H(\alpha)}{\frac{R_V^V(\alpha)}{FG} + \frac{R_H^V(\alpha)}{F} + \frac{R_V^H(\alpha)}{G}}\right]. \tag{36}$$

A plot of $I^U(\alpha)/I_0^U$ versus α is shown in figure 3. The points, O, represent values obtained by taking the data reported in table 1 and applying eq (36) with the average values of F and G reported in table 4. The solid line represents the theoretical curve which is obtained using eq (23a) with a value of $r = 0.383$ corresponding to the experimentally determined value of $D = 2.86$. As can be seen, $I^U(\alpha)/I_0^U$ does have a value of unity at 125.25° and 54.75° as predicted by Almgren [4] and Shinitzky [5] and approaches 0.90 at 90° and 1.2 at 180°. Similarly, eqs (21a) and (22a) can be written as

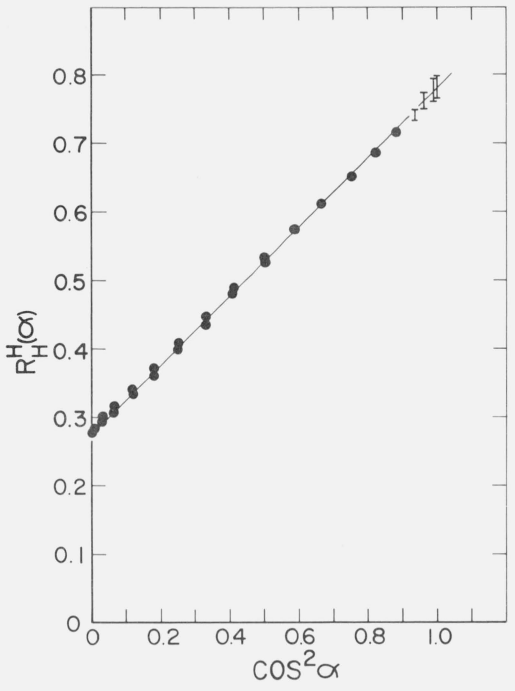

FIGURE 6. *Experimental readings,* $[R_H^H(\alpha)]$, *obtained with the excitation and emission polarizers in the horizontal position as a function of the* $\cos^2(\alpha)$ *where* α is the viewing angle.

The solid line refers to a least squares best fit of the data points.

$$\frac{I^V(\alpha)}{I_0^V} = (3/2)\left[\frac{R_V^V(\alpha)/G + R_H^V(\alpha)}{R_V^V(\alpha)/G + 2R_H^V(\alpha)}\right], \quad (37)$$

$$\frac{I^H(\alpha)}{I_0^H} = (3/2)\cos^2\alpha \left[\frac{R_H^H(\alpha) + R_V^H(\alpha)/G}{R_H^H(\alpha) + \frac{R_V^H(\alpha)}{G}(3\cos^2\alpha - 1)}\right]. \quad (38)$$

The data points on the $I^V(\alpha)/I_0^V$ and $I^H(\alpha)/I_0^H$ curves in figure 3 reflect the data recorded in tables 1 and 4 applied to eqs (37) and (38) while the solid lines are the theoretical curves given by eqs (21a) and (22a) for $r = 0.383$. The degree of polarization of the fluoresence emission can also be expressed in terms of the four readings and F and G. Equations (21b), (22b), and (23b) can be written in the forms

$$P^V(\alpha) = \left[\frac{R_V^V(\alpha)/G - R_H^V(\alpha)}{R_V^V(\alpha)/G + R_H^V(\alpha)}\right], \quad (39)$$

$$P^H(\alpha) = \left[\frac{R_V^H(\alpha)/G - R_H^H(\alpha)}{R_V^H(\alpha)/G + R_H^H(\alpha)}\right], \quad (40)$$

$$P^U(\alpha) = \frac{[R_V^V(\alpha)/FG + R_V^H(\alpha)/G] - [R_H^V(\alpha)/F + R_H^H(\alpha)]}{[R_V^V(\alpha)/FG + R_V^H(\alpha)/G] + [R_H^V(\alpha)/F + R_H^H(\alpha)]}. \quad (41)$$

Figure 4 shows plots of $P^V(\alpha)$, $P^H(\alpha)$, and $P^U(\alpha)$ as a function of α where the solid lines are calculated using $r = 0.383$ and eqs (21b), (22b), and (23b) respectively. The □, ○, and ● symbols refer to points obtained by applying the data in table 1 to eqs (39), (40), and (41) and again using the average values of F and G reported in table 4. As can be seen, the agreement with theory is good.

TABLE 4. *Calculated values of the polarization ratio for the detection system* (G), *the polarization ratio of the exciting radiation* (F), *and the dichroic ratio of emission* (D)

α Degrees	G	F	D
180	0.3524	1.023	2.845
144.75	.3558	1.019	2.827
125.25	.3551	1.014	2.853
90	.3512	1.002	2.879
54.75	.3515	1.008	2.874
180	.3535	1.016	2.853
160	.3551	1.025	2.841
80	.3501	1.000	2.887
Average	0.3531	1.013	2.857
Std. error	0.0007	0.003	0.007
% std. error	0.2	0.3	0.3

5.2. Excitation Polarizer Out, Emission Polarizer In

Since it was found that the exciting radiation is depolarized ($F = 1.013$), the $R_V(\alpha)$ and $R_H(\alpha)$ readings given in table 3 can be classified as $R_V^U(\alpha)$ and $R_H^U(\alpha)$, and expressed as

$$R_V^U(\alpha) = R_V^V(\alpha) + R_V^H(\alpha) = T_V[I_V^V(\alpha) + I_V^H(\alpha)] = kS^U T_V(\tau_{\parallel} + \tau_{\perp}), \quad (42a)$$

$$R_H^U(\alpha) = R_H^V(\alpha) + R_H^H(\alpha) = T_H[I_H^V(\alpha) + I_H^H(\alpha)] = kS^U T_H[\tau_{\parallel}\cos^2\alpha + \tau_{\perp}(2 - \cos^2\alpha)], \quad (42b)$$

where the superscript U denotes unpolarized excitation, and where $S^U = S^V = S^H$. Equation (42a) predicts that the $R_V(\alpha)$ readings in table 3 should be constant with respect to α and this was found to be true. The $R_H(\alpha)$ readings do change in accordance with eq (42b) as will be shown by obtaining expressions for $P^U(\alpha)$ and $I^U(\alpha)/I_0^U$. By combining eqs (42a) and (42b), $P^U(\alpha)$ can be expressed as

$$P^U(\alpha) = \left[\frac{R_V^U(\alpha)/G - R_H^U(\alpha)}{R_V^U(\alpha)/G + R_H^U(\alpha)}\right]. \quad (43)$$

TABLE 5. *Calculated and experimental values for the data obtained from four modes of spectrofluorimeter operation*

α Degrees	$\frac{I^U(\alpha)}{I_0^U}$	$\frac{I^U(\alpha)}{I^U(125.25°)}$[a]	$\frac{R^V(\alpha)}{R^H(\alpha)}$[b]		$\frac{I^U(\alpha)}{I_0^U}$	$\frac{R_U^U(\alpha)}{R_U^U(125.25°)}$[c]	$\frac{R(\alpha)}{R(125.25°)}$[d]	
	Eq (23a) Calc.	Eq (45) Expt.	Eq. (47) Calc.	Table 3 Expt.	Eq (23a) Calc.	Table 3 Expt.	Eq (50) Calc.	Table 3 Expt.
180	1.19	1.18	0.634	0.621	1.19	1.22	1.31	1.30
144.75	1.10	1.09	.785	.750	1.10	1.10	1.16	1.13
125.25	1.00	1.00	1.03	.983	1.00	1.00	1.00	1.00
90	0.905	0.913	1.50	1.48	0.905	0.903	0.846	0.855
54.75	1.00	1.01	1.03	1.01	1.00	1.00	1.00	1.06

[a] Polarizer in emission beam, no polarizer in the excitation beam.
[b] Polarizer in excitation beam, no polarizer in the emission beam.
[c] Both beams depolarized.
[d] No polarizers or depolarizers in either beam.

The points, ▲, on the $P^U(\alpha)$ curve in figure 4 reflect eq (43) applied to the $R_V(\alpha)$ and $R_H(\alpha)$ data in table 3 for a value of $G=0.353$ as in the previous section. At any viewing direction α, the total intensity received by the detection system is

$$I^U(\alpha) \propto R_V^U/G + R_H^U. \tag{44}$$

If the exciting light is unpolarized, then by eq (23b) $I^U(125.25°)$ or $I^U(54.75°)=I_0^U$. Therefore, the prediction is that

$$\frac{I^U(\alpha)}{I_0^U}=\frac{I^U(\alpha)}{I^U(125.25°)} = \left[\frac{R_V^U(\alpha)/G+R_H^U(\alpha)}{R_V^U(125.25°)/G+R_H^U(125.25°)}\right]. \tag{45}$$

A comparison of $I^U(\alpha)/I_0^U$ values as calculated using eq (23a) and a value of $r=0.383$ with $I^U(\alpha)/I^U(125.25°)$ values as calculated using eq (45) with the $R_V(\alpha)$ and $R_H(\alpha)$ data in table 3 and a value of $G=0.353$, is shown in table 5. In this comparison as well as the $P^U(\alpha)$ one, the agreement of the data with the theoretical values using eqs (23a) and (23b) is good, thus showing the validity of eqs (42a), (42b), (44), and (45) in describing the data. An even more rigorous test of eq (23a) would be when G as well as F has a value of unity. This will be shown in the section dealing with depolarized beams.

5.3. Excitation Polarizer In, Emission Polarizer Out

In this mode of operation the two readings $R^V(\alpha)$ and $R^H(\alpha)$ can be described as

$$R^V(\alpha) = R_V^V(\alpha) + R_H^V(\alpha) = kS^V(\tau_{||}T_V + \tau_\perp T_H)$$

$$= T_V I_V^V(\alpha) + T_H I_H^V(\alpha), \tag{46a}$$

$$R^H(\alpha) = R_V^H(\alpha) + R_H^H(\alpha) = kS^H[\tau_\perp T_V + (\tau_{||}\cos^2\alpha + \tau_\perp \sin^2\alpha)T_H]$$

$$= T_V I_V^H(\alpha) + T_H I_H^H(\alpha)\cdot \tag{46b}$$

Equation (46a) predicts that the $R^V(\alpha)$ readings should be constant with respect to α. Actually, the values increase slightly from 180° to 54.75° indicating that the beam was slightly displaced from the entrance slit of the emission monochromator when the emission polarizer was removed, so that the solid angle collected by the detection system changed slightly with α. However, the $R^H(\alpha)$ reading should also suffer the same effect and by taking the ratio of the two readings, the effects should cancel. No attempt was made to re-aline the optics for fear of changing F and G. This ratio is

$$\frac{R^V(\alpha)}{R^H(\alpha)}=F\left[\frac{(\tau_{||}T_V+\tau_\perp T_H)}{(\tau_{||}\cos^2\alpha+\tau_\perp\sin^2\alpha)T_H+\tau_\perp T_V}\right]$$

$$=\left[\frac{F(DG+1)}{(D-1)\cos^2\alpha+(G+1)}\right]. \tag{47}$$

Taking D, F, and G from table 4, the right side of eq (47) can be calculated and compared to the ratio $R^V(\alpha)/R^H(\alpha)$. This IS done in table 5 and the agreement is good. Equations (46a) and (46b) do not lend themselves to giving information on $P^U(\alpha)$ or $I^U(\alpha)/I_0^U$ easily and no attempt will be made to do so. Equation (47), however, proved very useful when alining the scrambler plates as will be shown in the next section.

5.4. Both Beams Depolarized

In order to remove the bias of the detection system, scrambler plates were placed in the emission beam. When this was done, it was found that the readings obtained were extremely sensitive to the alinement of the scrambler. This was also found by Rahn, Temple, and Hathaway [13] and Reed and Lendon [14]. To accomplish alinement it was necessary to put the excitation polarizer back in the system and place the

emission detection system at 180°. Under these conditions eq (47) becomes

$$\frac{R^V(180°)}{R^H(180°)}=\frac{F(DG+1)}{(G+D)} \tag{48}$$

The scrambler plates were then rotated and adjusted such that the $R^V(180°)$ reading equaled the $R^H(180°)$ reading. Since in this case F is essentially equal to unity, G must now also equal unity so as to satisfy eq (48). The excitation polarizer was then removed and readings, $R_U^U(\alpha)$, were taken at various angles α (see table 3). Since $F=G=1$, eq (23a) now applies and the experimentally obtained ratios of $R_U^U(\alpha)/R_U^U(125.25°)$ should agree with the calculated ratio $I^U(\alpha)/I_0^U$ as given by eq (23a) for the experimentally obtained value $r=0.383$. The comparison is shown in table 5 and shows the validity of Almgren [4] and Shinitzky's [5] predictions once the instrumental polarization artifacts (i.e., F and G) are eliminated.

Equation (23a) can be written as

$$r=\left[\frac{R_U^U(\alpha)}{R_U^U(125.25°)}-1\right]\left[\frac{4}{(3\cos^2\alpha-1)}\right], \tag{49}$$

and thus shows that r can be measured from $R_U^U(\alpha)$ readings at different viewing angles. For example at $\alpha=90°$, the value of $R_U^U(90°)/R(125.25°)$ is 0.903, giving a value of $r=0.388$ which is in fair agreement with a value of $r=0.383$ as given by the analysis with polarizers placed in the system. Thus we have the novel situation of being able to measure the anisotropy (or polarization) of a sample without using polarizers. It should be noted, however, that this type of measurement is extremely sensitive to small alinement errors as can be seen by eq (49). Thus, the best ratio to use is $R_U^U(180°)/R_U^U(125.25°)$. However, the $R_U^U(180°)$ measurement suffers from scattered exciting light problems and requires a fairly large blank subtraction. The next best set of angles to use is then $R_U^U(90°)$ and $R_U^U(125.25°)$.

5.5. No Polarizers or Scramblers

When there are no polarizers or depolarizers in the system, the reading, $R(\alpha)$, taken at each viewing angle α, can be described theoretically by eq (27). The reading R_0 that one would obtain if the emission anisotropy, r, were equal to zero cannot be measured independently. However, eq (27) can be tested by taking the ratio

$$\frac{R(\alpha_1)}{R(\alpha_2)}$$

$$=\frac{(1+F)(1+G)+r[3\cos^2\alpha_1-(1+F+G-2FG)]}{(1+F)(1+G)+r[3\cos^2\alpha_2-(1+F+G-2FG)]} \tag{50}$$

of any two $R(\alpha)$ readings. Table 5 shows a comparison of the ratios $R(\alpha)/R(125.25°)$ obtained from the appropriate data in table 3 to that calculated using eq (50) with $r=0.383$, $F=1.013$ and $G=0.353$. As can be seen the agreement is good and this supports the validity of eq (27) in describing the error introduced into the system by polarization effects. The limiting values for the relative error, $R(\alpha)/R_0$, can be obtained by assuming the maximum and minimum values that F, G, and r can obtain. Some examples are given in table 6. For the cases where $F=G=1$, the

TABLE 6. *Theoretical estimates of errors, $R(\alpha)/R_0$, which can be introduced into fluorescence measurements by polarization effects*

α Degrees	r	F	G	$R(\alpha)/R_0$	Comments
90	0.4	1.0	1.0	0.90	absorption dipole || to
180	0.4	1.0	1.0	1.20	emission dipole.
125.25	0.4	1.0	1.0	1.00	
90	−0.2	1.0	1.0	1.05	absorption dipole ⊥ to
180	−0.2	1.0	1.0	0.90	emission dipole.
125.25	−0.2	1.0	1.0	1.00	
90	0.4	10^4	10^4	1.80	R_V^V absorption || to emission
90	0.4	10^4	10^{-4}	0.60	R_H^V
90	0.4	10^{-4}	10^4	0.60	R_V^H
90	0.4	10^{-4}	10^{-4}	0.60	R_H^H
180	0.4	10^4	10^4	1.80	R_V^V absorption || to emission
180	0.4	10^4	10^{-4}	0.60	R_H^V
180	0.4	10^{-4}	10^4	1.80	R_V^H
180	0.4	10^{-4}	10^{-4}	0.60	R_H^H
90	−0.2	10^4	10^4	0.60	R_V^V absorption ⊥ to emission
90	−0.2	10^4	10^{-4}	1.20	R_H^V
90	−0.2	10^{-4}	10^4	1.20	R_V^H
90	−0.2	10^{-4}	10^{-4}	1.20	R_H^H
180	−0.2	10^4	10^4	0.60	R_V^V absorption ⊥ to emission
180	−0.2	10^4	10^{-4}	1.20	R_H^V
180	−0.2	10^{-4}	10^4	0.60	R_V^H
180	−0.2	10^{-4}	10^{-4}	1.20	R_H^H
90	0.4	3.0	0.3	0.808	absorption || to emission;
180	0.4	3.0	0.3	1.04	excitation in U.V., emission
125.25	0.4	3.0	0.3	0.885	in red
90	−0.2	3.0	0.3	1.10	absorption ⊥ to emission;
180	−0.2	3.0	0.3	0.981	excitation in U.V., emission
125.25	−0.2	3.0	0.3	1.06	in red
90	0.4	3.0	2.8	1.26	absorption || to emission;
180	0.4	3.0	2.8	1.34	excitation in U.V., emission
125.25	0.4	3.0	2.8	1.29	in U.V.
90	−0.2	3.0	2.8	0.868	absorption ⊥ to emission;
180	−0.2	3.0	2.8	0.829	excitation in U.V., emission
125.25	−0.2	3.0	2.8	0.855	in U.V.
90	0.4	0.33	0.3	0.669	absorption || to emission;
180	0.4	0.33	0.3	1.36	excitation red, emission
125.25	0.4	0.33	0.3	0.90	in red
90	−0.2	0.33	0.3	1.16	absorption ⊥ to emission;
180	−0.2	0.33	0.3	0.819	excitation in red, emission
125.25	−0.2	0.33	0.3	1.05	in red

limits of Almgren [4], Shinitzky [5], and Kalantar [10] are obtained. The cases where F and G are very large or very small correspond to the cases where polarizers are placed in the emission and excitation beams. Finally, there are the cases where there are no polarizers (or scrambler plates) in the beams and the values of F and G run roughly from 2 to 3 in the UV to 0.2 to 0.3 in the red. In these cases, values of F and G are essentially determined by the polarization properties of the excitation and emission monochromators. Some of these cases are also given in table 6.

6. Conclusions

Errors introduced in fluorescence measurements by polarization effects can be quite large. In addition to the cases mentioned by Shinitzky [5], there are others in which polarization effects can introduce errors. Relative fluorescence quantum yield measurements where either or both the sample or reference have a degree of polarization will be susceptible to polarization errors [4, 5, 10]. Relative quantum yields measured as a function of temperature, especially at low temperatures where the viscosity of the solvent changes drastically, may have polarization errors since the emission anisotropy of the fluorescence is strongly dependent on the viscosity of the solvent. Also, quantum counters such as rhodamine B in ethylene glycol may exhibit a degree of polarization which is a function of α, r, F, and G, the most important being r which is a function of the dye and F which is a function of the excitation monochromator and beam splitter. These parameters will vary as the excitation wavelength changes. Another case where polarization effects can be large is in measuring relative fluorescence to phosphorescence ratios which are usually performed using low temperature glasses as solvents. Again the signal is a function of α, r, F, and G but in this case G will change drastically as one scans over the fluorescence and phosphorescence emission envelopes.

In general it can be said that in making fluorescence measurements, one should either polarize completely or depolarize completely since it is not known whether polarization effects are introducing errors until either the degree of polarization is determined or the effect is negated. If there is a nonzero degree of polarization, the readings will be a function of r, α, F, and G. The effects of these parameters can then be either (a) measured accurately by placing polarizers in both beams, thus completely describing the measuring system or (b) negated by placing depolarizing elements in both beams and measuring the signal at one of the 'depolarizing' angles 54.75° or 125.25°. With polarizers in both beams, more information is obtained; i.e., r, G, F, and R_0 can be calculated using the four readings at any viewing angle α. In this case, however, four scans must be made, which may be difficult if the sample is photochemically unstable. With depolarizers in both beams, 54.75° or 125.25° viewing must be used to measure R_0 and no information is obtained on r unless viewing is performed at another angle (e.g., 90°). Even so, the measurement of r in this way is more sensitive to small alinement errors than when r is determined using polarizers. One could use polarizers in addition to depolarizers to measure r at the 54.75° or 125.25° viewing angles, but this complicates the optics and, of course, is more expensive since a good set of depolarizers costs as much as a good set of polarizers. A distinct disadvantage in using depolarizers is the fact that 54.75° or 125.25° viewing must be used whereas most commercial fluorimeters are right angle viewing—a geometry preferred for use with polarizers. It should be mentioned that whichever one uses, polarizers or depolarizers, they must be efficient over a wide wavelength range. Also, since they are optical components their spectral sensitivity must be accounted for when calibrating the instrument to give corrected spectra. Considering all these factors, the recommended procedure is to use two polarizers (with right angle viewing as used by Azumi and McGlynn [2] for most applications), and obtain F, G, r, and R_0 directly from the four readings. This has the advantage that all four parameters are measured with the same solution and sample cell under conditions of constant optics and alinement. This is important since F is a function of the excitation optics up to and including the sample cell and G is a function of the total emission detection system which also includes the sample cell. Thus, r and I_0 are parameters of the solution only.

Finally, some recommendations for fluorescence standards can now be made. The recommendations made by Melhuish [3] and others that ideal fluorescence standards should be depolarized is confirmed here. If there are cases, however, in which a certain compound or solution has distinct advantages as a fluorescence standard even though it does exhibit a degree of polarization, the emission anisotropy, r, of the standard (a fundamental parameter of the system) should be measured as a function of wavelength and reported. The user can then refer to the appropriate equations listed in the theoretical section to determine I_0 or R_0 and the degree of polarization P that the standard will have under his experimental conditions.

7. References and Notes

[1] Weber, G., and Teale, F. W. J., Trans. Faraday Soc. **53**, 646 (1957).
[2] Azumi, T., and McGlynn, S. P., J. Chem. Phys. **37**, 2413 (1962).
[3] Melhuish, W. H., J. Res. Nat. Bur. Stand. (U.S.) **76A**, (Phys. and Chem.), No. 6, 547–560 (Nov.–Dec. 1972).
[4] Almgren, M., Photochem. and Photobiol. **8**, 231 (1968).
[5] Shinitzky, M., J. Chem. Phys. **56**, 5979 (1972).
[6] A summary of previous derivations of polarization equations is given by E. N. Hudson in Fluorescence Spectroscopy, Eds. A. J. Pesce, C.-G. Rosén and T. L. Pasby (M. Dekker, Inc., New York, 1971), pp. 111–130.
[7] The units for photon quantities used in this paper are those recommended by J. J. Muray, F. E. Nicodemus, and I. Wunderman, Appl. Opt. **10**, 1465 (1971).
[8] Berlman, I. B., in Handbook of Fluorescence Spectra of Aromatic Molecules (Academic Press, New York, 1971), 2d ed., pp. 18, 19.
[9] Jablonski, A., Acta. Phys. Polon. **16**, 471 (1957).
[10] Kalantar, A. H., J. Chem. Phys. **48**, 4992 (1968).

[11] In order to describe materials and experimental procedures adequately, it is occasionally necessary to identify commercial products by manufacturer's name or label. In no instances does such identification imply endorsement by the National Bureau of Standards, nor does it imply that the particular product or equipment is necessarily the best available for that purpose.

[12] Mielenz, K. D., to be published.
[13] Rahn, L., Temple, P., and Hathaway, C., Appl. Spectry. **25,** 675 (1971).
[14] Reed, P., and Lendon, D., Appl. Spectry. **26,** 489 (1972).

(Paper 79A1–842)